AIP Journal of Applied Physics

# Low-temperature copper-induced lateral growth of polycrystalline germanium assisted by external compressive stress

Bahman Hekmatshoar, Shams Mohajerzadeh, Davood Shahrjerdi, Ali Afzali-Kusha, Michael D. Robertson, and Aaryn Tonita

Citation: Journal of Applied Physics **97**, 044901 (2005); doi: 10.1063/1.1836012
View online: http://dx.doi.org/10.1063/1.1836012
View Table of Contents: http://scitation.aip.org/content/aip/journal/jap/97/4?ver=pdfcov
Published by the AIP Publishing

**Articles you may be interested in**
Effect of bilayer geometry on the diffusion of Ni in amorphous Si and the consequent growth of silicides
J. Vac. Sci. Technol. B **30**, 061203 (2012); 10.1116/1.4757134

Hydrogenation-assisted nanocrystallization of amorphous silicon by radio-frequency plasma-enhanced chemical vapor deposition
J. Appl. Phys. **100**, 104320 (2006); 10.1063/1.2390629

Stress-assisted nickel-induced crystallization of silicon on glass
J. Vac. Sci. Technol. A **22**, 966 (2004); 10.1116/1.1722271

Low temperature crystallization of germanium on plastic by externally applied compressive stress
J. Vac. Sci. Technol. A **21**, 752 (2003); 10.1116/1.1569923

Large-grain polycrystalline silicon films with low intragranular defect density by low-temperature solid-phase crystallization without underlying oxide
J. Appl. Phys. **91**, 2910 (2002); 10.1063/1.1448395

AIP Journal of Applied Physics

*Journal of Applied Physics* is pleased to announce André Anders as its new Editor-in-Chief

[This article is copyrighted as indicated in the article. Reuse of AIP content is subject to the terms at: http://scitation.aip.org/termsconditions. Downloaded to ] IP: 216.165.95.70 On: Tue, 26 Aug 2014 20:00:06

HTML ABSTRACT + LINKS



# Low-temperature copper-induced lateral growth of polycrystalline germanium assisted by external compressive stress

Bahman Hekmatshoar, Shams Mohajerzadeh,[a] Davood Shahrjerdi, and Ali Afzali-Kusha
*Thin Film Laboratory, Department of Electrical and Computer Engineering, University of Tehran, Tehran, Iran*

Michael D. Robertson and Aaryn Tonita
*Department of Physics, Acadia University, Wolfville, Nova Scotia, B4P 2R6, Canada*

(Received 18 December 2003; accepted 1 November 2004; published online 20 January 2005)

Copper-induced lateral growth of polycrystalline germanium (poly-Ge) at temperatures as low as 150 °C was enabled by the application of an external mechanical stress during the annealing step of sample processing. An equivalent compressive strain of 0.05% was externally applied at 150 °C for 10 h to a deposited amorphous Ge layer and crystalline growth rates of 2.5 and 1.8 $\mu$m/h were observed in directions parallel and perpendicular to the stress axis, respectively. These results were confirmed by scanning electron microscope and transmission electron microscopy (TEM) analyses. In addition, TEM and x-ray diffraction analyses indicate that a fraction of poly-Ge annealed in the presence of applied compressive stress possessed a tetragonal structure with space-group $P4_32_12$. The presence of the tetragonal phase is hypothesized to be the primary mechanism responsible for the lateral growth of poly-Ge. © *2005 American Institute of Physics*. [DOI: 10.1063/1.1836012]

## I. INTRODUCTION

Crystallization of semiconductor layers is an important process governing the final performance of electronic devices and the demands of industry for low manufacturing cost have driven crystallization technologies towards low thermal budget processes. In addition, low-temperature processes are necessary in applications involving low-temperature flexible substrates, such as polymeric films, of interest in some display technologies and reel-to-reel fabrication methods. Since the driving capability of thin-film transistors (TFTs) required for flexible displays is directly proportional to carrier mobility, there is a requirement for a high-quality, polycrystalline semiconductor layer.

One technique known to reduce the crystallization temperature of semiconductors is the metal-induced crystallization (MIC),[1] where metals are either alloyed with the semiconductor or layered adjacent to the semiconductor and the structure is annealed to promote crystallization. Aluminum-induced crystallization of germanium has been widely investigated by forming multilayers of Al/Ge.[2–4] Although MIC involving high levels of Al reduces the crystallization temperature of Ge to as low as 100 °C, the semiconductor properties are severely degraded by metal contamination and the grown poly-Ge layer possesses prohibitively low mobilities for high-performance devices. Similarly, Cu-MIC of Ge has been proposed as an alternative approach for developing poly-Ge with low metal contamination, but the annealing temperature required to achieve crystallization is as high as 400 °C.[5,6]

In order to further reduce the crystallization temperature and decrease the metal contamination, we have recently devised a stress-assisted, Cu-induced crystallization technique for Ge. This method not only reduces the level of metal contamination to less than 1 at. % but is achieved at annealing temperatures as low as 130 °C,[7] The decrease in the annealing temperature is achieved by the presence of mechanical compressive stress externally applied to the flexible polyethylene terephthalate (PET) substrate during the annealing step. One potential drawback to this technology is the introduction of cracks into the structure from the applied compressive stress. However, by proper patterning of the amorphous Ge layer before thermomechanical posttreatment, the stress-induced crack density in the Ge layer can be minimized or eliminated, allowing for efficient device fabrication.[8]

A fundamental problem inherent to all MIC techniques is the incorporation of metal into the semiconductor layer. In order to reduce the adverse effects associated with metal contamination in the active layer in silicon-based devices, the Si may be encouraged to crystallize in a direction lateral to the metal-covered region. This technique is known as metal-induced-lateral crystallization (MILC) and has been observed for the lateral growth of poly-Si from a nickel-seeded region.[9,10] Another important advantage of MILC is the controlled growth of polycrystalline material with grain boundaries longitudinally oriented to the desired current flow. This contrasts MIC where the grain boundaries are randomly distributed[11,12] and there is no preferential direction for current flow. Since longitudinal grain boundaries do not impede the flow of electrons parallel to the boundaries, higher carrier mobility is expected in the MILC approach.

In this paper, we report the lateral crystallization of germanium from a copper-seeded germanium region at annealing temperatures as low as 150 °C enabled by the application of an external mechanical stress during annealing. The polycrystalline grains are oriented, thereby realizing improvements in carrier mobility, as discussed above for MILC

[a]Electronic mail: smohajer@vlsi.uwaterloo.ca

 © 2005 American Institute of Physics

[This article is copyrighted as indicated in the article. Reuse of AIP content is subject to the terms at: http://scitation.aip.org/termsconditions. Downloaded to ] IP: 216.165.95.70 On: Tue, 26 Aug 2014 20:00:06

of silicon. Our experiments indicate that the application of external mechanical stress is a necessary condition and annealing at temperatures up to 400 °C in the absence of mechanical stress does not lead to lateral crystallization of Ge. This technique is a promising candidate for low-temperature processes that require device-quality semiconductors, such as high-mobility TFTs in flexible display applications.

## II. EXPERIMENT

The substrates used during the growth experiments were flexible, 100-$\mu$m-thick PET films which maintain flexibility at temperatures below 180 °C. At higher temperatures, PET undergoes thermal degradation and the films become brittle. A 1000-Å-thick layer of amorphous germanium (*a*-Ge) was deposited directly onto the PET substrates by an e-beam evaporation at a base pressure of $10^{-6}$ Torr and a substrate temperature of 100 °C and was followed by an e-beam deposition of a 2000-Å-thick $SiO_2$ passivation layer at the same temperature. After patterning the $SiO_2$ layer by means of standard photolithography methods, a 100-Å Cu layer was deposited by thermal evaporation ensuring that the Cu could not diffuse into regions of Ge still covered by $SiO_2$. The sacrificial $SiO_2$ layer was removed by a lift-off technique leaving Cu-seeded islands on the *a*-Ge layer and the samples were subjected to the thermomechanical posttreatment at an annealing temperature of 150 °C for 10 h. The mechanical compressive stress was applied during annealing by bending the flexible PET substrates inward and the radius of the inward curvature was set to exert an equivalent compressive strain of 0.05% to the *a*-Ge layer.

X-ray diffraction results were acquired using a Philips X'Pert MPD Pro system using a copper target. The accelerating potential of the incident electrons was 40 kV, the current was 50 mA, and monochromated Cu $K\alpha$ x ray was used. All of the scanning electron microscope (SEM) images were obtained on an XL30 Philips system using secondary electrons (SEs) to highlight surface features. Plan-view specimens for a transmission electron microscopy (TEM) investigation were prepared by a low-angle polishing at about 1° using the MultiPrep™ polishing system from Allied High Tech.[13] The TEM study was performed using a Philips EM301 transmission electron microscope operated at 100 kV and low beam currents in order to minimize the degradation of the PET substrate.

## III. RESULTS AND DISCUSSION

Figure 1(a) presents a SEM image of the lateral growth of poly-Ge for a sample patterned in squares using a standard photolithography. The copper-seeded region is located within the two rectangular boundaries and the lateral growth of the Ge is observed at both the inner and outer edges of the copper-seeded rim as dark bands. A higher magnification SEM image of one of the corners of the copper-seeded region is shown in Fig. 1(b). The lateral crystallization growth rates are anisotropic, and from this image, a growth rate of 2.5 $\mu$m/h is observed in the direction of the external stress axis whereas a lower rate of 1.8 $\mu$m/h is observed in the direction perpendicular to the stress axis. We believe that

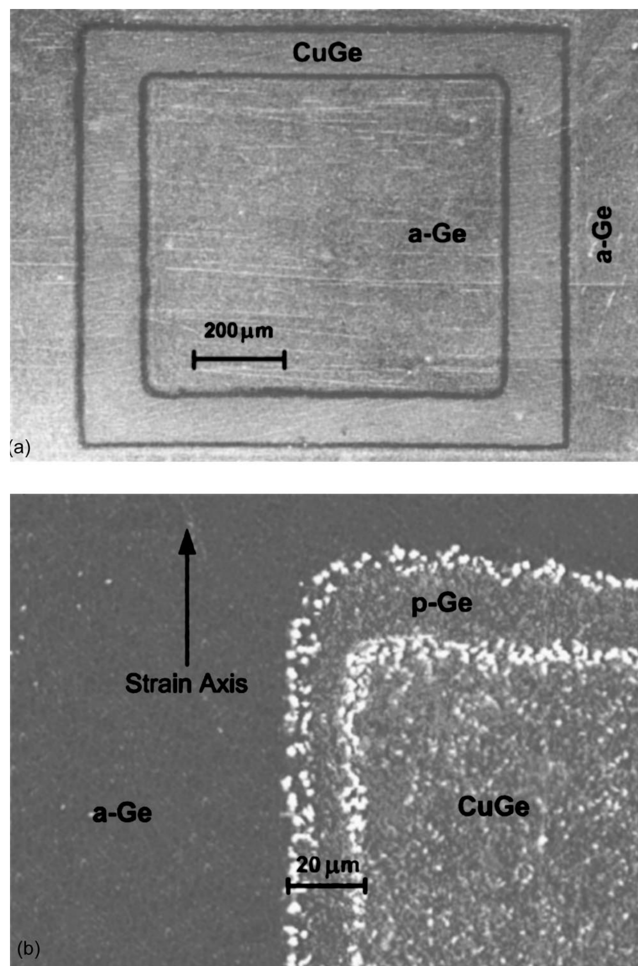


FIG. 1. SEM micrographs taken by (SEs), showing (a) a square pattern exposed to a compressive stress during lateral crystallization and (b) higher magnification of the corner, indicating a difference in lateral-growth rate in directions parallel and perpendicular to the external stress.

such orientational effects may be attributed to the nature of the PET substrate, which transfers the external mechanical stress to the Ge layer via the interface. Similar to other polymers, PET may have either biaxial or uniaxial orientations, depending on the production method. However, most of the commercially available PET films are uniaxially oriented[14] and may affect the conduction and transfer of stress fields in the polymer. In addition, it has been verified that applying mechanical strain changes the direction or alignment of the polymer crystallites especially in the direction of the uniaxial strain even if there is no annealing.[15] So orientational effects might be aggravated during annealing in the presence of compressive stress and exhibit orientation-dependent characteristics.

Figure 2(a) presents a low-magnification secondary electron SEM image displaying three distinct regions: Cu-seeded germanium (CuGe), laterally grown poly-germanium (*p*-Ge), and the remaining amorphous germanium (*a*-Ge). The three distinct regions of the sample can be further delineated by etching with a weak ammonia solution for 10-20 s, as shown in the higher magnification image of Fig. 2(b), and the lateral growth of the germanium layer from the copper–germanium polycrystalline seed layer is suggested.

[This article is copyrighted as indicated in the article. Reuse of AIP content is subject to the terms at: http://scitation.aip.org/termsconditions. Downloaded to ] IP: 216.165.95.70 On: Tue, 26 Aug 2014 20:00:06

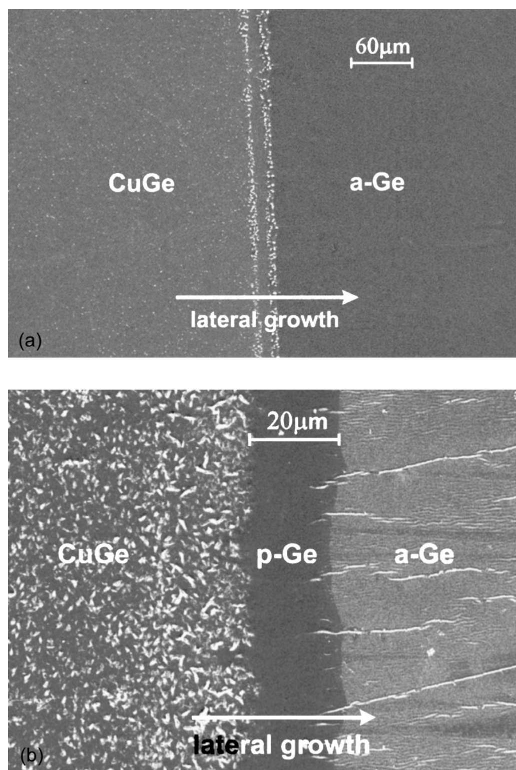


FIG. 2. SEM micrographs of a sample (a) before and (b) after being etched in an ammonia solution, taken by (SEs). The three regions of Cu-seeded Ge, lateral-growth strip, and the remaining *a*-Ge are discernible in the graph. The width of the lateral-growth strip is 20 $\mu$m.

As observed in the SEM micrograph presented in Fig. 2(b), the applied stress can lead to the formation of buckling sites and cracks in the *a*-Ge regions of the sample. We have observed that by the proper patterning of the *a*-Ge layer before the thermomechanical posttreatment, the formation of the buckling and cracking sites can be minimized or eliminated.[7,8] Specifically, by making the *a*-Ge layer no wider than about 50–100 $\mu$m in the direction of the applied stress, depending on the orientation of the PET substrate, complete elimination of the cracks can be achieved.

The surface morphology of the lateral-growth region is depicted in the SEM image of Fig. 3 and a granular surface morphology with grains oriented in the direction of the lateral-growth axis is observed. This surface morphology is typical of laterally grown crystallites and provides evidence for the polycrystalline nature of this region. The orientation of the polycrystals was not observed in the nonlaterally grown regions of the specimen.

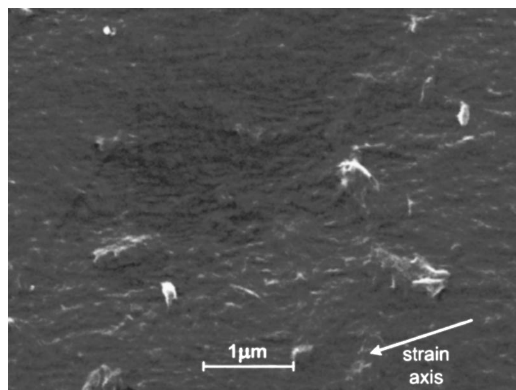


FIG. 3. SEM micrograph showing the surface morphology of a portion of the lateral-growth strip. The micrograph is taken by (SEs).

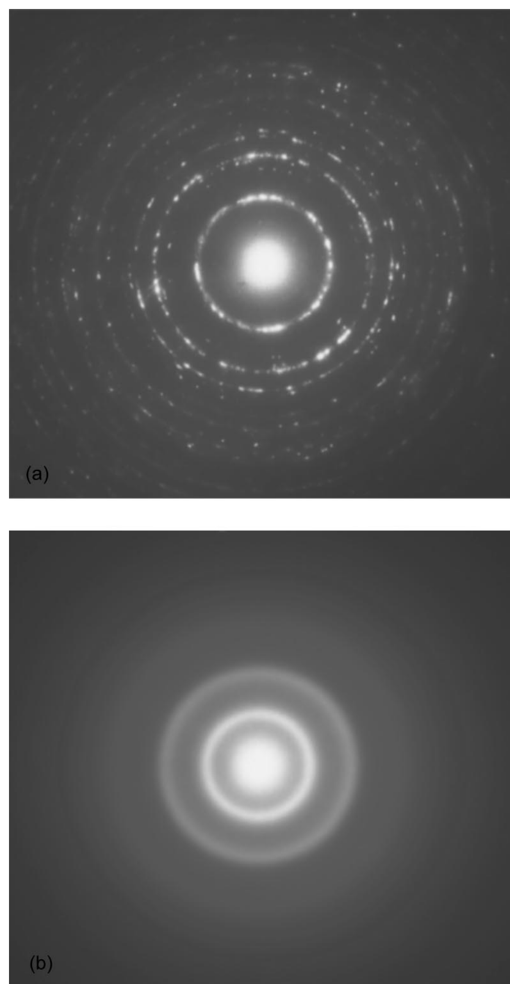


FIG. 4. TEM selected area diffraction patterns of (a) the laterally grown and Cu-seeded poly-Ge regions and (b) the amorphous region.

TEM analysis has also been performed to study the crystallinity of the poly-Ge layer. Presented in Figs. 4(a) and 4(b) are selected area diffraction patterns (SADPs) where the diffraction aperture was located over the copper-seeded/lateral-growth and amorphous Ge regions of the sample, respectively. The well-defined rings of spots shown in the SADP of Fig. 4(a) are characteristic of a polycrystalline material. Conversely, the *a*-Ge region only displays diffuse rings characteristic of amorphous material, confirming that crystallization is limited to areas at the vicinity of the copper–germanide seeds. Figure 5 is an enlarged image of the upper left-hand quadrant of the SADP shown in Fig. 4(a) and diffraction rings up to cubic-Ge {113} have been labeled from 1 to 16 for clarity. Table I summarizes the indices assigned to these rings based on the measured and theoretical ratios of the diameter of the diffraction rings, using the *c*-Ge {111} diffraction ring as an internal reference, for cubic-Ge (*c*-Ge), tetragonal-Ge (*t*-Ge), and monoclinic copper germanide ($Cu_3Ge$). A lattice parameter of $a=5.66$ Å was used for *c*-Ge;[16] $a=5.93$ Å and $c=6.93$ Å for *t*-Ge with 12 atoms per

[This article is copyrighted as indicated in the article. Reuse of AIP content is subject to the terms at: http://scitation.aip.org/termsconditions. Downloaded to ] IP: 216.165.95.70 On: Tue, 26 Aug 2014 20:00:06

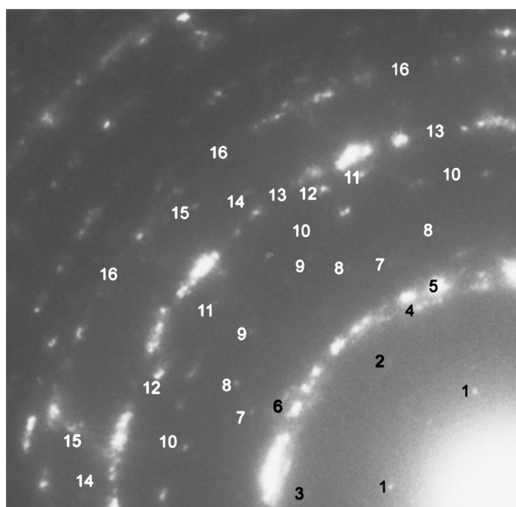


FIG. 5. An enlargement of the upper left-hand quadrant of Fig. 4(a) with the first 16 polycrystalline rings labeled.

unit cell and space-group $P4_32_12$;[17] and $a$=2.631 Å, $b$ =4.200 Å, $c$=4.568 Å, and $\beta$=81°41′ for monoclinic $Cu_3Ge$.[18] The quantities in parentheses in the second column of the table represent two-standard deviation (95%) uncertainties in the measured values. The existence of three different structures in this sample is confirmed by the unique indexing of many of the diffraction rings: rings 5 and 6 for *c*-Ge; rings 1, 3, 4, 7, 9, and 15 for *t*-Ge; and rings 6, 11, and 14 for $Cu_3Ge$. All of the significant diffraction spots, as suggested by the calculated electron structure factors, have been included in Table I.

TABLE I. Summary of electron-diffraction results. The values in parentheses ( ) denote two-standard deviation uncertainty values in the measured reciprocal spacing.

| Ring No. | Measured reciprocal spacing ($nm^{-1}$) | Assignment | Theoretical reciprocal spacing ($nm^{-1}$) |
|---|---|---|---|
| 1 | 1.62 (0.06) | *t*-Ge {100} | 1.68 |
| 2 | 2.48 (0.06) | *t*-Ge {110} | 2.39 |
| | | $Cu_3Ge$ {010} | 2.39 |
| 3 | 2.72 (0.09) | *t*-Ge {111} | 2.78 |
| 4 | 2.88 (0.09) | *t*-Ge {002} | 2.88 |
| 5 | 3.06 (0.09) | *c*-Ge {111} | 3.06 |
| 6 | 3.21 (0.09) | $Cu_3Ge$ {011} | 3.24 |
| 7 | 3.37 (0.09) | *t*-Ge {102} | 3.34 |
| | | *t*-Ge {200} | 3.37 |
| 8 | 3.76 (0.09) | *t*-Ge {112} | 3.73 |
| | | *t*-Ge {201} | 3.67 |
| | | $Cu_3Ge$ {100} | 3.82 |
| 9 | 4.04 (0.09) | *t*-Ge {121} | 4.04 |
| 10 | 4.35 (0.09) | *t*-Ge {202} | 4.44 |
| | | $Cu_3Ge$ {002} | 4.41 |
| 11 | 4.56 (0.09) | $Cu_3Ge$ {110} | 4.53 |
| 12 | 4.74 (0.09) | *t*-Ge {220} | 4.77 |
| | | $Cu_3Ge$ {101} | 4.68 |
| 13 | 4.93 (0.09) | *c*-Ge {220} | 4.99 |
| | | $Cu_3Ge$ {012} | 5.02 |
| 14 | 5.23 (0.09) | $Cu_3Ge$ {222} | 5.26 |
| 15 | 5.66 (0.09) | *t*-Ge {222} | 5.66 |
| 16 | 5.84 (0.09) | *c*-Ge {113} | 5.88 |

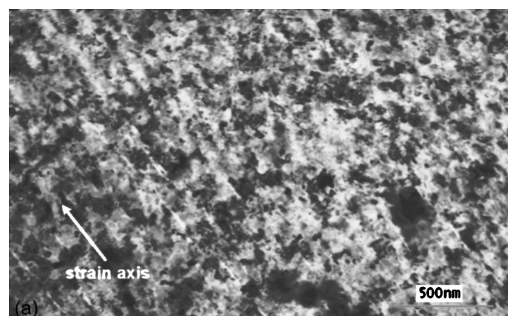


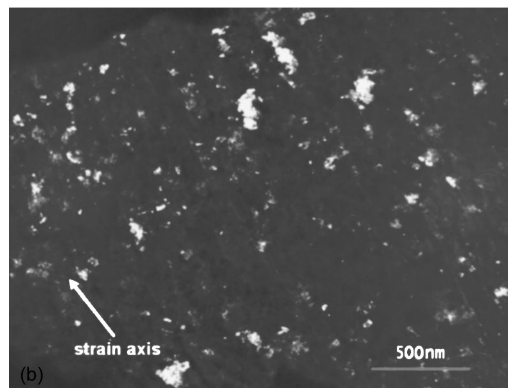


FIG. 6. Plan-view TEM images of the lateral-growth region: (a) bright field and (b) dark field. For the dark-field image, the objective aperture with a diameter of 0.75 $nm^{-1}$ in reciprocal space, was positioned over the *c* -Ge{111} diffraction ring.

Bright and dark-field TEM diffraction contrast images of the laterally grown regions of the film are given in Figs. 6(a) and 6(b), respectively. The size of the crystals ranges from tens to hundreds of nanometers and the crystallites are elongated and aligned in the direction of lateral growth.

The XRD spectrum of the Cu-seeded Ge regions is presented in Fig. 7(b) and shows a diffraction peak at 23.2°, indexed as *t*-Ge 110, and is attributed to the partial growth of poly-Ge in a tetragonal atomic structure. In addition, the 220 peak of *c*-Ge is observed in the figure, but the 111 peak of *c*-Ge is buried beneath the large peak of the partially crystalline PET substrate. The 110 *t*-Ge peak was only observed when the samples underwent mechanical stress during the thermal posttreatment. The spectrum of Fig. 7(a) shows the result of a poly-Ge layer prepared on glass by means of Cu-MIC at 400 °C and no evidence of tetragonal distortion is observed.[19] In addition, bare PET substrates were subjected to thermomechanical posttreatment at similar conditions to ensure that the diffraction peak at 23.2° was not generated by a phase transition in PET and was confirmed by the spectrum presented in Fig. 7(c).

In order to investigate the microscopic mechanism of the stress-assisted lateral-growth phenomenon, identical Cu-seeded Ge samples were prepared on PET and glass and annealed without the application of an external stress. In all cases, there was no sign of lateral growth, even at annealing temperatures as high as 400 °C. It is hypothesized that the compressive stress produces a local tetragonal distortion of the cubic Cu-seeded poly-Ge islands and these regions are

[This article is copyrighted as indicated in the article. Reuse of AIP content is subject to the terms at: http://scitation.aip.org/termsconditions. Downloaded to ] IP: 216.165.95.70 On: Tue, 26 Aug 2014 20:00:06

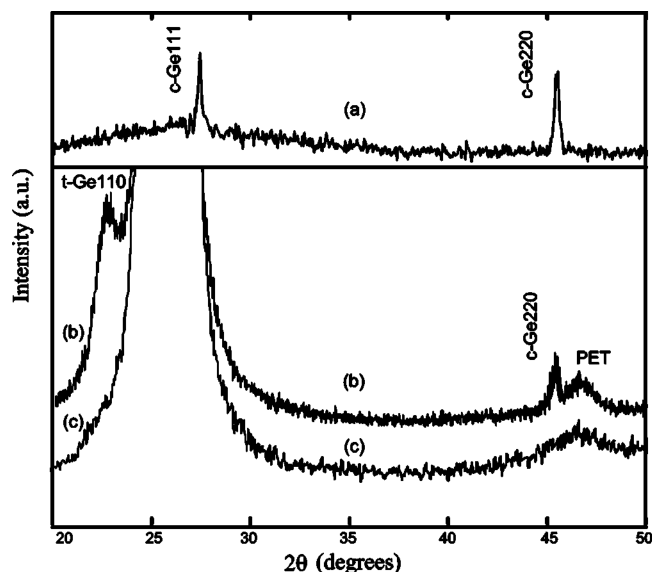


FIG. 7. An XRD spectrum of (a) poly-Ge prepared by Cu-MIC at 400 °C on a glass substrate with no stress, (b) the Cu-seeded poly-Ge region prepared in the presence of compressive stress, where the 110 peak of *t*-Ge is discernible, and (c) bare PET subjected to thermomechanical treatment.

crystallized during the thermomechanical posttreatment. From the literature, there is some evidence that *c*-Ge crystallites may undergo a partial phase transition to a tetragonal structure during epitaxial growth on Si wafers as a result of the stress induced by the lattice mismatch between the Si and Ge layers. As the thickness of the grown Ge layer is increased, the lattice mismatch is aggravated and leads to the enhancement of the phase transition.[20,21] This phase transition is believed to be due to the preferential nucleation of higher-pressure phases with a higher packing density of atoms under high-stress conditions. In this way, compressive stress is partially relaxed by a more dense arrangement of Ge atoms in the crystal lattice. A similar mechanism may account for the observed phase transition in poly-Ge in the presence of mechanical compressive stress. Thus, it is proposed that a stress-induced-tetragonal-crystallization mechanism is responsible for the lateral growth of polycrystalline Ge from copper-seeded Ge crystallites.

## IV. SUMMARY AND CONCLUSION

In summary, we have presented a stress-assisted, Cu-induced lateral-crystallization technique for the preparation of polycrystalline Ge on flexible PET substrates at temperatures as low as 150 °C. The surface morphology and crystallinity of the lateral-growth region have been studied and confirmed by SEM and TEM analyses. TEM and XRD analyses have been also performed to address the microscopic functionality of compressive stress to the partial phase transition of *c*-Ge to the *t*-Ge structure. This crystallization approach may enable technologies requiring low processing temperatures, such as the fabrication of TFT drivers for flexible displays and plastic microelectronics, to access higher-quality TFTs with mobilities much greater than those possible, based on amorphous semiconductor structures.

[1] T. Missana, C. N. Ofonso, A. K. Petford-Long, and R. C. Doole, Appl. Phys. Lett. **69**, 2039 (1996).
[2] T. J. Konno and R. Sinclair, Mater. Sci. Eng., A **179**, 426 (1994).
[3] I. Konvács, O. Gestzi, P. Harmat, and G. Radnóczi, Phys. Status Solidi A **161**, 153 (1997).
[4] F. Katsuki, K. Hanafusa, and M. Yonemora, J. Appl. Phys. **89**, 4643 (2001).
[5] J. P. Doyle, B. G. Svensson, and S. Johanson, Appl. Phys. Lett. **67**, 2804 (1995).
[6] A. Khakifirooz, S. S. Mohajerzadeh, S. Haji, and E. Asl Soleimani, Mater. Res. Soc. Symp. Proc. **618**, 255 (2000).
[7] B. Hekmatshoar, D. Shahrjerdi, S. Mohajerzadeh, A. Khakifirooz, A. Goodarzi, and M. Robertson, J. Vac. Sci. Technol. A **21**, 752 (2003).
[8] B. Hekmatshoar, D. Shahrjerdi, S. Mohajerzadeh, A. Khakifirooz, A. Akhavan, and M. Robertson, Mater. Res. Soc. Symp. Proc. **769**, 183 (2003).
[9] S. W. Lee and S. K. Joo, IEEE Electron Device Lett. **17**, 160 (1996).
[10] G. A. Bhat, Z. Jin, H. S. Kwok, and M. Wong, IEEE Electron Device Lett. **20**, 167 (1999).
[11] G. A. Bhat, Z. Jin, H. S. Kwok, and M. Wong, IEEE Electron Device Lett. **20**, 97 (1999).
[12] V. W. C. Chan and P. C. H. Chan, IEEE Trans. Electron Devices **49**, 1399 (2002).
[13] Y. Leterrier, L. Boogh, J. Andersons, and J. A. E. Manson, J. Polym. Sci., Part B: Polym. Phys. **35**, 1449 (1997).
[14] K. C. Cole, H. Ben Daly, B. Sanschagrin, K. T. Nguyen, and A. Ajji, Polymer **40**, 3505 (1999).
[15] P. M. Voyles, J. L. Grazul, and D. A. Muller, Ultramicroscopy **96**, 251 (2003).
[16] K. W. Böer, *Survey of Semiconductor Physics: Electrons and Other Particles in Bulk Semiconductors* (Van Nostrand Reinhold, New York, 1990), p. 127.
[17] J. A. Vergés, M. Alouani, and N. E. Christensen, Phys. Rev. B **38**, 1378 (1988).
[18] M. O. Aboelfotoh and H. M. Tawancy, J. Appl. Phys. **75**, 2441 (1994).
[19] A. Khakifirooz, S. Haji, S. S. Mohajerzadeh, R. Shafiiha, and E. A. Soleimani, Sens. Mater. **14**, 67 (2002).
[20] S. Sato, S. Nozaki, H. Morisaki, and M. Iwase, Appl. Phys. Lett. **66**, 3176 (1995).
[21] J. L. Xu, J. L. Chen, and J. Y. Feng, Nucl. Instrum. Methods Phys. Res. B **194**, 297 (2002).

[This article is copyrighted as indicated in the article. Reuse of AIP content is subject to the terms at: http://scitation.aip.org/termsconditions. Downloaded to ] IP: 216.165.95.70 On: Tue, 26 Aug 2014 20:00:06